# A comparative study of carrot root tissue colonization and cell wall degradation by *Pythium violae* and *Pythium ultimum*, two pathogens responsible for cavity spot

**C. Campion, B. Vian, M. Nicole, and F. Rouxel**

**Abstract**: The process of infection of carrots by *Pythium violae* and *Pythium ultimum*, two causes of cavity spot, is described. The first species causes limited root necrosis, the second progressive root rot. Colonization by both species was intracellular and limited within the tissues. Modes of cell wall degradation were studied by staining (PATAg test) and labeling techniques. Pectins were labeled with monoclonal antibodies and cellulose with an exoglucanase–gold complex. Cell wall polysaccharides were degraded differently by the two species. *Pythium violae* was responsible for degradations, which could be noticeable, especially for high methylesterified pectins, but which occurred after colonization and were localized near the hyphae. The conservation of integrity of diseased tissue was apparently due to the absence of degradation away from the hyphae. In contrast, *P. ultimum* was responsible for more extensive degradation of pectins and cellulose, which occurred at a relatively greater distance from the hyphae. Degradation of pectins was always more rapid in the cell walls than in the intercellular junctions. This phenomenon led to loss of tissue integrity and could explain the tissue maceration caused by *P. ultimum* infection. These differences in infection process are discussed in connection with the enzymic potential for degradation of cell wall polysaccharides.

*Key words*: *Daucus carota* L., *Pythium*, pectin, cellulose, cytochemistry.

**Résumé** : Nous décrivons le développement de l'infection chez la carotte par *Pythium violae* et *Pythium ultimum,* deux agents de la maladie de la tache évolutive. L'espèce *P. violae* cause une nécrose restreinte des racines et *P. ultimum* est responsable d'une tache des racines. Ces deux espèces ont une croissance intracellulaire et limitée dans les tissus. Les modes de dégradation de la paroi cellulaire ont été étudiés par coloration (épreuve PATAg) et par marquage. Les pectines ont été marquées avec des anticorps monoclonaux et de la cellulose avec un complexe exoglucanase–or. Les polysaccharides de la paroi cellulaire ne sont pas dégradés de la même façon par ces deux espèces. *Pythium violae* est responsable de dégradations qui peuvent être observées au niveau des pectines fortement méthylestérifiées, mais ces dégradations surviennent après la colonisation et sont localisées près des hyphes. Le tissu malade conserve son intégrité ce qui pourrait s'expliquer par une absence de dégradation à distance des hyphes. *Pythium ultimum* est de son côté responsable d'une dégradation plus poussée des pectines et de la cellulose qui se produit relativement plus loin des hyphes. La dégradation des pectines est toujours plus rapide dans les parois cellulaires que dans les jonctions intercellulaires. Ce phénomène entraîne la perte de l'intégrité des tissus et pourrait expliquer la macération des tissus observée lors de l'infection par *P. ultimum*. Ces différences dans le processus infectieux sont discutées en fonction du potentiel enzymatique de dégradation des polysaccharides de la paroi cellulaire.

*Mots clés* : *Daucus carota* L., *Pythium*, pectine, cellulose, cytochimie.
[Traduit par la rédaction]

## Introduction

Cavity spot is one of the most prejudicial diseases on carrots, causing severe yield losses and above all depreciation in quality (Montfort and Rouxel 1988). Evidence for biological origin of this root disorder was provided by Groom and Perry (1985) then by White (1988) who established that two slow-growing *Pythium* species, *P. violae* and *P. sulcatum*, were the major fungal species responsible for the disease in Europe. Recently,

Received August 18, 1997. Revision received December 15, 1997. Accepted December 16, 1997.

**C. Campion**[1] **and F. Rouxel.** Station de pathologie végétale, Institut National de la Recherche Agronomique, B.P. 29, 35653, Le Rheu Cedex, France.
**B. Vian.** Laboratoire de pathologie végétale, Institut National Agronomique Paris-Grignon, 16, rue Claude Bernard, 75231, Paris Cedex 05, France.
**M. Nicole.** Laboratoire de phytopathologie, Office de la Recherche Scientifique et Technique Outre-Mer, 911, avenue d'Agropolis, B.P. 5045, 34032, Montpellier, France.

[1] Author to whom all correspondence should be addressed.



the role of several fast-growing *Pythium* species was also demonstrated (Guérin et al. 1994; El-Tarabily et al. 1996), including *P. ultimum*, which is one of the cavity spot-causing agents in the United States (Vivoda et al. 1991).

Although superficial, cavity spot symptoms vary, depending on the *Pythium* species group involved in their development. *Pythium violae* is responsible for limited necrosis (Groom and Perry 1985), whereas the development of symptoms caused by *P. ultimum* is more progressive, with a water-soaked aspect (Campion et al. 1997), leading to the question of the existence of diverse mechanisms for pathogenesis.

Only few data are available about the infection process and the mode of degradation of carrot cell walls by *P. violae* and *P. ultimum*. Groom and Perry (1985) provided evidence for colonization of the periderm and secondary phloem parenchyma by *P. violae* and for cell collapse in the secondary phloem parenchyma. More recently, the degradation pattern of carrot cell walls by *P. violae* was associated with the production of in situ fungal enzymes that altered cell wall polysaccharides (Zamski and Peretz 1996). In vitro, secretion of cellulase, pectate lyase, and possibly protopectinase by this species was demonstrated to be weak and late (Campion et al. 1997), raising the question of relationships between hydrolase activities and the limited symptoms observed on carrots.

In contrast, *P. ultimum* is known to have a high potential for degradation of cell wall polysaccharides in vitro, since it can secrete polygalacturonase, pectin lyase, cellulase, and possibly protopectinase in relatively high amounts (Campion et al. 1997). Colonization of carrot tissues and in situ secretion of cell wall polysaccharide-degrading enzymes by *Pythium* spp. are poorly documented.

This study reports on changes in carrot root cell walls after infection by *P. violae* or *P. ultimum*. Using different staining and immunolabeling procedures, colonization of the root tissues by the two pathogens, as well as degradation of cell wall polysaccharides, including pectins and cellulose, were cytochemically examined. Considering that carrot cell walls are particularly rich in pectins (Kirtschev et Kratchanov 1980), the degree of alteration of these molecules likely would be of importance for the changes in tissue cohesion (Collmer and Keen 1986).

## Materials and methods

### Sample preparation and embedding for light and electron microscopy

Healthy carrot roots (Nanco cultivar) were obtained after growing for 4 months in a steam-sterilized mixture of soil, sand, and peat (1:1:1, by volume) and placed in a glasshouse maintained at 15–20°C. After harvesting, carrot roots were washed in tap water and inoculated following the method described by Montfort and Rouxel (1988): each root freshly wounded with an abrasive sheet was inoculated with four mycelial agar plugs from the edge of a 5-day-old colony grown at 20°C on a carrot juice – agar medium (200 mL of carrot juice centrifuged for 20 min with 2.5% $CaCO_3$, 20 g of agar, and 800 mL of deionized water). Inoculation was performed with two *Pythium* isolates, *P. violae* 20 and *P. ultimum* 185, isolated from cavity spot lesions on carrot roots in the field and maintained at the Station de pathologie végétale, Institut National de la Recherche Agronomique (Le Rheu, France). Roots on which agar plugs free from mycelium had been deposited were used as controls.

Samples of 2 $mm^3$ (1 $mm^2$ area at the surface of the lesion and 2 mm depth in the tissue) were collected from the lesions obtained after 2 or 4 days of incubation at 20°C or from the tissues close to the agar plug for the controls. The samples were fixed for 2 h in a 4% v/v glutaraldehyde solution in 0.1 M cacodylate–HCl buffer (pH 7.2), washed twice, and immersed overnight in the buffer. After postfixation for 1 h in a 1% w/v osmium tetroxide solution in the same buffer and thorough rinsing, samples were dehydrated by a 1-h immersion in a graded series of ethanol (30, 50, 70, 95, and 100% v/v). Samples were then embedded in LR White resin (medium grade, The London Resin Co. Ltd.) by immersion for at least 4 h in graded resin–alcohol mixtures (25, 50, and 75% v/v) then in pure resin. Polymerization was carried out overnight at 58°C.

### Toluidine blue staining

Semithin sections were stained with toluidine blue (0.5% w/v in 2.5% w/v $Na_2CO_3$), rinsed, mounted in water or air dried, and then mounted in Eukitt medium (Kindler GmbH and Cie, Freiburg, Germany), before observation with a light microscope (Leitz, Dialux 22).

### Periodic acid – thiosemicarbazide – silver proteinate test for the detection of polysaccharides

Ultrathin sections collected on gold grids were stained with the periodic acid – thiosemicarbazide – silver proteinate (PATAg) test (Thiéry 1967). The sections were floated on a 1% w/v periodic acid solution for 30 min and then rinsed twice for 10 min in distilled water. They were maintained for 4 h on a 0.2% w/v thiosemicarbazide solution in 20% v/v acetic acid, washed in progressively decreasing acetic acid concentration solutions and then in pure water. The sections were treated with 1% w/v silver proteinate for 30 min in the dark. Grids were thoroughly rinsed then air dried before examination with a Philips CM 12 transmission electron microscope operating at 80 kV. Grids floated on distilled water or in 1% v/v $H_2O_2$ solution instead of periodic acid solution were used as controls.

### Immunogold labeling of pectic substances

Immunogold labeling was performed using the monoclonal antibodies JIM 5 and JIM 7, anti-homogalacturonic sequences, kindly provided by Dr. K. Roberts (John Innes Centre, Norwich). JIM 5 recognizes low methylesterified sequences (VandenBosch et al. 1989), whereas JIM 7 permits detection of high methylesterified ones (Knox et al. 1990).

*Light microscopy*

Semithin sections collected on multiwell glass slides were first floated in a moist chamber on 0.01 M phosphate buffer saline (PBS; pH 7.4), containing 0.5% w/v bovine serum albumin, 0.15 M NaCl, and 1% v/v Tween 20. After 10 min, sections were treated for 30 min in a solution of normal goat serum diluted 1:30 in the same buffer, then they were treated for 4 h at room temperature or overnight at 4°C with JIM 5 or JIM 7 diluted 1:4 in the same buffer. Sections were rinsed three times for 10 min in PBS, then treated with a solution of goat anti-rat immunoglobulin conjugated with 5-nm colloidal gold particles (EM.GAT 5, British Biocell International) diluted 1:30 in PBS. After rinsing five times in the buffer and twice in distilled water, sections were dried and the gold labeling was intensified with the Silver Enhancement Kit (British Biocell International). After exactly 4 min, sections were thoroughly rinsed and eventually stained with toluidine blue. Next, they were air dried and mounted in Eukitt medium before observation under a light microscope with bright field or epipolarized (filter Zeiss, A Pol. 487960) light (De Mey et al. 1986).

*Transmission electron microscopy*

Ultrathin sections were treated for double-labeling with JIM 5 and JIM 7. The procedure was the same as for light microscopy except that sections were treated with 0.01 M Tris–HCl buffer (pH 7.4) and silver intensification was not used. Grids were first treated on one side with JIM 5 (or JIM 7) and a solution of anti-rat immunoglobulin

conjugated with 5-nm diameter gold particles (EM.GAT 5, British Biocell International). Grids were then treated on the other side with JIM 7 (JIM 5 for grids already treated with JIM 7), using the same procedure and a solution of anti-rat immunoglobulin conjugated with 15-nm diameter colloidal gold particles (EM.GAT 15, British Biocell International). Next, grids were stained with uranyl acetate and eventually lead citrate before observation with a Philips CM 12 transmission electron microscope operating at 80 kV.

For both light and electron microscopy, controls were prepared by omitting the incubation of the sections with JIM 5 and JIM 7, or by replacing this step by incubation with solutions of the first antibody previously incubated with its antigen for 2 h at room temperature (JIM 5 diluted 1:4 in a solution of 1 mg sodium pectate·mL$^{-1}$ or JIM 7 diluted 1:4 in a solution of 1 mg pectin·mL$^{-1}$ in PBS or Tris–HCl buffer).

### Enzyme-gold labeling of β-1,4-glucans

Labeling of β-1,4-glucans was performed using an exoglucanase – colloidal gold complex, prepared as described by Benhamou et al. (1987). Ultrathin sections collected on nickel grids were floated for 10 min at 25°C on a drop of 0.01 M PBS (pH 6.5) containing polyethylene glycol. After drying, they were incubated for 20 min in a moist chamber with the enzyme–gold complex diluted 1:2 in PBS. They were rinsed thoroughly in 0.01 M PBS (pH 7.2) and then in distilled water. Sections were stained with uranyl acetate and lead citrate before examination with a Philips CM 12 transmission electron microscope operating at 80 kV.

## Results

### Histological observations of external tissues from infected carrot root

After infection by *P. violae*, colonization was limited to the periderm, the pericyclic parenchyma, and superficial cell layers of the secondary phloem parenchyma, reaching 350 µm deep from the root surface (Fig. 1). Hyphae were seen intracellularly and walls of infected cells presented swelling and a loss of staining with toluidine blue. These changes were observed in cells of the secondary phloem parenchyma only. Swelling was particularly noticeable at sites where hyphae were seen crossing the cell walls (Fig. 2), but no apparent modification in the tissue integrity was observed.

Differences in infection after inoculation by *P. ultimum* were noted mainly in the cell wall degradation pattern. Although the pathogen was found in the same tissues (Fig. 3), alteration of walls was not limited to the immediate vicinity of the fungus as judged by the considerable swelling and loss of staining in the infected areas. In swollen cell walls, only intercellular junctions remained apparently undegraded and highly stained (Fig. 4). These modifications led to loss of cell cohesion and tissue integrity, 96 h after inoculation (data not shown).

### Changes in cell wall texture revealed by the PATAg test

After infection by *P. violae*, the PATAg test revealed degradations of varying intensity: some cell walls remained compact and evenly stained (as for the control, data not shown) (Fig. 5), whereas other cell walls were highly swollen. In this case, observations revealed a multilayered organization of portions of swollen cell walls where the middle lamella was seen to be locally PATAg negative (Fig. 6).

After infection by *P. ultimum*, highly swollen cell walls throughout also displayed a multilayered organization as revealed by PATAg staining (Figs. 7 and 8). Cell wall changes were observed both close to and at a distance from *P. ultimum* hyphae and the PATAg staining remained intense only in intercellular junctions (Fig. 7). Partly degenerated *P. ultimum* hyphae were often observed in the infected tissues (Fig. 8).

### Changes in pectic polysaccharides revealed by immunolabeling using monoclonal antibodies

In healthy tissues, cell walls and intercellular junctions were regularly labeled with JIM 5 (Fig. 9) and JIM 7 monoclonal antibodies. Labeling was proportionally more intense after the use of JIM 5 than after JIM 7, whatever the order of application of the two antibodies, especially over limited areas of the middle lamella (Fig. 10).

In carrot roots infected by *P. violae*, sections treated with JIM 5 or with JIM 7 displayed an intense labeling over undegraded cell walls but a weak labeling over swollen ones. This result was observed by comparing toluidine blue staining by bright field and immunogold labeling by epipolarized light observation (Figs. 11 and 12). Labeling was absent over wall portions where hyphae were located. At the ultrastructural level, double labeling using JIM 5 and JIM 7 was poor or absent over areas close to hyphae, where often only labeling with JIM 5 occurred (Fig. 13).

After infection by *P. ultimum*, cell walls were unevenly labeled with JIM 5 in the transition zone between infected and healthy tissues. Toluidine blue staining and pectin labeling were lacking over highly swollen cell walls, except over intercellular junctions (Figs. 14, 15, 16, 17, 18, and 19). The labeling was uneven over irregularly swollen cell walls but regular over undegraded cell walls at the limit of the infected zone (Figs. 15 and 16). After the use of JIM 5 and JIM 7 monoclonal antibodies, labeling was seen over similar areas, but labeling with JIM 5 was particularly intense over intercellular junctions. Over partially swollen intercellular junctions, the labeling was uneven, almost absent over the less electron-opaque portion and intense over the more intense electron-opaque portion (Fig. 19). The limit between these two areas was very sharp, showing a less intense labeling over primary cell walls than over the internal portion of the intercellular junction. No significant labeling was observed over *P. violae* and *P. ultimum* hyphae or over sections from the control material.

### Changes in β-1,4-glucans using an exoglucanase–gold complex

After labeling of sections from healthy tissues with the exoglucanase–gold complex the probe, gold particles were found to be evenly but weakly distributed over primary cell walls (Fig. 20). After infection with *P. violae*, detection of β-1,4-glucans was stronger over slightly swollen cell walls than over cell walls in the healthy material, particularly close to hyphae (Fig. 21). Treatments of sections from carrot roots infected with *P. ultimum* showed that labeling was regular over highly swollen cell walls (Figs. 22 and 23) or over less electron-opaque portions of intercellular junctions (Fig. 24). Gold particles were sometimes distributed linearly in swollen cell walls (Fig. 23). β-1,4-Glucans were also detected over cell walls of the two *Pythium* species, as judged by the intense labeling (Fig. 21).

## Discussion

Colonization of carrot roots by both *P. violae* and *P. ultimum* resulted from an intracellular progression of hyphae associated

**Figs. 1–4.** Aspects of the carrot root external tissues colonized by *P. violae* or *P. ultimum*, 48 h after inoculation (toluidine blue staining, bright field microscope observations). P, periderm; Pp, pericyclic parenchyma; Pl, secondary phloem parenchyma. Figure 1 is a low magnification of tissues showing intense colonization of periderm cells, pericyclic parenchyma cells, and superficial cell layers of the secondary phloem parenchyma by *P. violae*. Hyphae are mainly intracellular (arrows). Secondary phloem parenchyma cell walls are swollen locally and stained differently by toluidine blue (arrowhead), compared to unaltered areas. Scale bar = 50 µm. Figure 2 is an enlargement of Fig. 1 showing the swollen cell walls. Swelling is particularly noticeable around hyphae passing through the cell wall; it displays a loss in toluidine blue staining. Scale bar = 10 m. Figure 3 is a low magnification of tissues showing cell colonization by *P. ultimum* in the superficial cell layers of the secondary phloem parenchyma. Note the sharp limit between altered and unaltered tissues. Hyphae are mainly intracellular (arrow). Plant cell walls are highly swollen and slightly stained by toluidine blue, as compared to cells of unaltered areas (arrowhead). Scale bar = 50 µm. Figure 4 is a detail of Fig. 3 showing considerable swelling along the whole cell walls; the intercellular junctions remain undegraded and strongly stained (arrows). Scale bar = 10 µm.

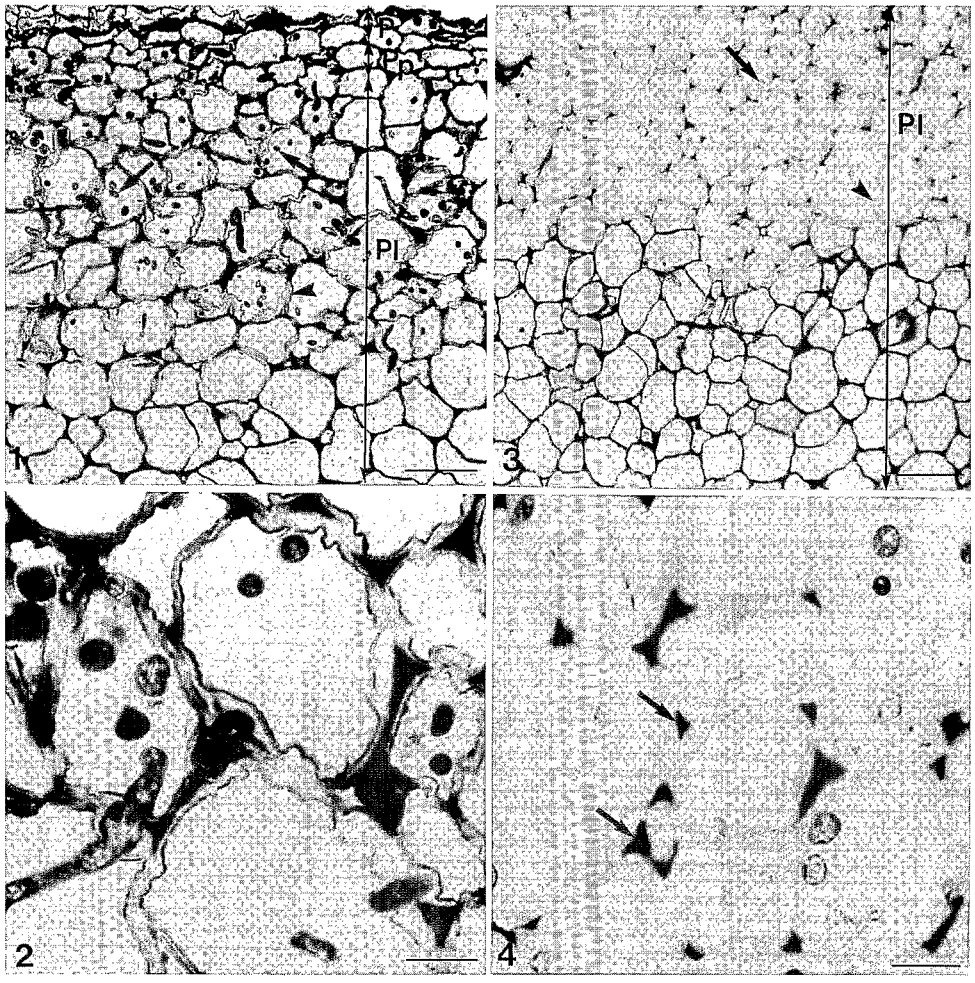


with cell wall penetration. This phenomenon, previously described for *P. violae* by Briard (1990) and Guérin (1993), was established here for the first time for *P. ultimum*. Hyphae were seen in outer root tissues, i.e., the periderm, the pericyclic parenchyma, and external cell layers of the secondary phloem parenchyma, but cell wall changes were observed in the secondary phloem parenchyma only. From these observations, we hypothesize that induction of cell wall polysaccharide-degrading enzymes occurred only after the colonization of several cell layers, as was suggested by Chérif et al. (1991) for infection of cucumber by *P. ultimum*. The diffusion of enzymes within the infected tissues seemed to be limited, since cell wall changes were never observed beyond the fungal colonization line. These observations are in agreement with the limited development of symptoms induced by the two *Pythium* species in the superficial root tissues and contrast with results obtained for other carrot pathogens such as *Botrytis cinerea,* which was responsible for cell wall degradation before penetration of carrot tissues (Sharman and Heale 1977), and *Mycocentrospora acerina*, which degraded carrot walls ahead of the mycelium colonization line (Le Cam et al. 1997).

In our study, pectic substances were heavily labeled in healthy carrot tissues. Low methylesterified substances were always seen in greater quantity than high methylesterified ones, mainly in the middle lamella and intercellular junctions, as mentioned for carrot tissues and other material by Vanden-Bosch et al. (1989) and Knox et al. (1990). This result may be judged inconsistent, since the degree of methylesterification of

**Figs. 5–8.** Ultrastructural aspects of the cell walls in the secondary phloem parenchyma of carrot roots infected by *P. violae* or *P. ultimum*, 96 h after inoculation (PATAg staining, transmission electron microscope observations). W, plant cell wall; H, hypha; J, intercellular junction; ML, middle lamella. Scale bars = 1 μm. Figure 5 is a micrograph showing a slightly swollen cell wall close to a *P. violae* hypha, where the PATAg reactivity remains regular. Figure 6 shows that in cells colonized by *P. violae* hyphae, the walls have a multilayered organization (arrow). Locally, the middle lamella is PATAg negative (arrowhead). Figures 7 and 8 show that in cells infected by *P. ultimum*, cell walls display highly swollen areas with a multilayered aspect. The PATAg staining remains even in the intercellular junctions (Fig. 7, arrows). Note the occurrence of degenerated hyphae close to a swollen cell wall (Fig. 8).

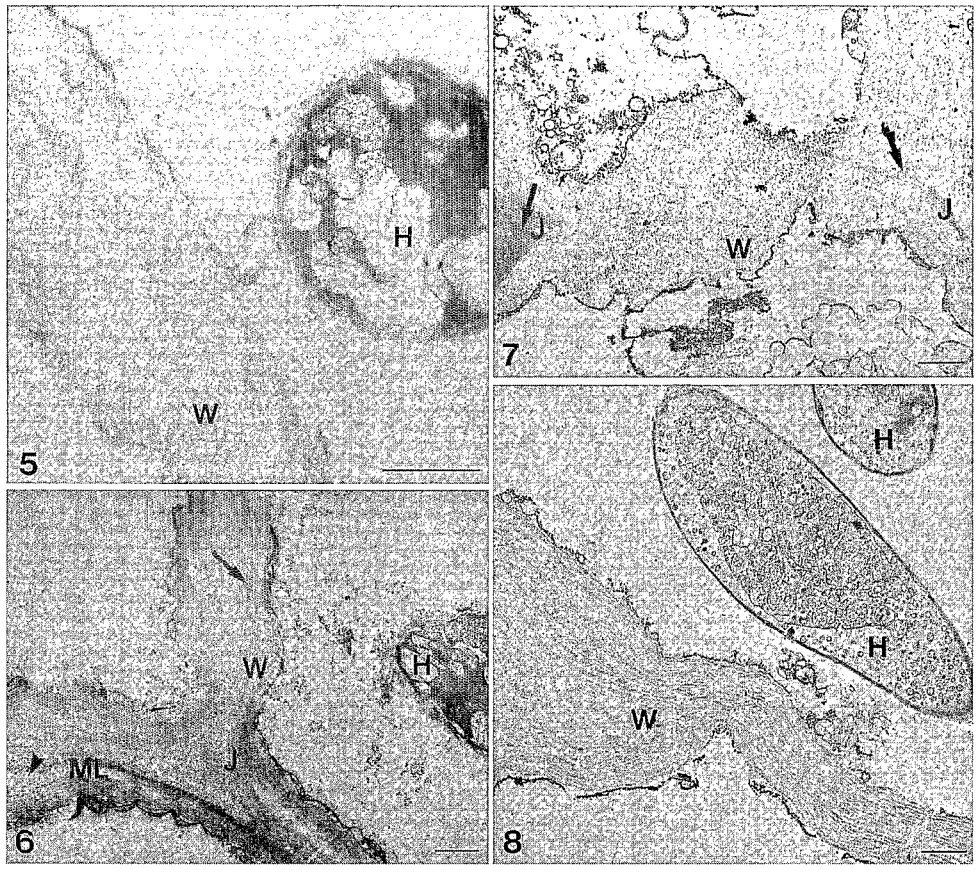


carrot root pectins was described as high (about 70%, Massiot et al. 1988), but it suggests that low methylesterified zones of pectins are more accessible to monoclonal antibodies than high methylesterified ones. In contrast, cellulose was slightly detected in cell walls in healthy tissues, probably because cellulose chains did not display numerous affinity sites for the exoglucanase–gold probe.

After infection of carrot roots, *P. violae* degraded host cell walls but in limited areas near the hyphae. This limited degradation may explain why the integrity of the infected tissues was maintained up to 4 days after inoculation and why symptoms had a dry aspect. No cavity was observed in *P. violae* infected tissues, in agreement with results obtained by Briard (1990), who reported that the cavity formation occurred 8 days after infection. The limited degradation owing to *P. violae* may be related to the weak enzymic potential for cell wall polysaccharide degradation previously established in vitro (Campion et al. 1997) and in situ (Zamski and Peretz 1996). However, *P. violae* was capable of degrading pectic substances. This degradation was apparently greater for high methylesterified pectins than for low methylesterified ones, suggesting the activity of a pectin methylesterase on carrot pectins as detected in other plants, such as cherry tomato (Roy et al. 1992) or bean (Deising et al. 1996). Though no pectin methylesterase was detected in vitro for *P. violae* (Campion 1997), we hypothesized that this enzyme was secreted only in planta or in undetectable amounts in vitro.

Solubilization of middle lamella associated with the development of *P. violae* may be attributed to the pectate lyase detected in vitro (Campion et al. 1997). The supposition of the role of this enzyme in our model is reinforced by the fact that such a solubilization was observed by treatment with a pure endopectate lyase from *Erwinia chrysanthemi* on cell walls of rice (Baker et al. 1980).

Modification in labeling of cellulose after infection suggests that this polymer was more accessible to the probe because of partial degradation of pectins or that it was altered by *P. violae* in situ. Though exo-β-1,4-glucanases may be produced by *P. violae*, the increase in labeling suggests that endo-β-1,4-glucanase or cellobiohydrolase activity is present in situ, releasing free extremities along the cellulose chains (Henrissat et al. 1985; Touzani and Donèche 1996).

*Pythium ultimum* was responsible for a strong modification in parenchyma integrity, resulting in greater and more

**Figs. 9 and 10.** Immunodetection of pectins in the cell walls of secondary phloem parenchyma in healthy carrot material. W, plant cell wall; ML, middle lamella. Figure 9 shows immunogold labeling with JIM 5, silver enhancement and epipolarized light observation. The bright signal appears regularly distributed in cell walls and middle lamellae. Scale bar = 10 μm. Fig. 10 shows a cell wall labeled with JIM 5 (large particles, 15 nm) and JIM 7 (small particles, 5 nm) (uranyl acetate and lead citrate staining). Both gold particles are evenly distributed over the whole cell wall, but labeling is more intense with JIM 5 over some areas of the middle lamella (arrow). Scale bar = 0.5 μm.

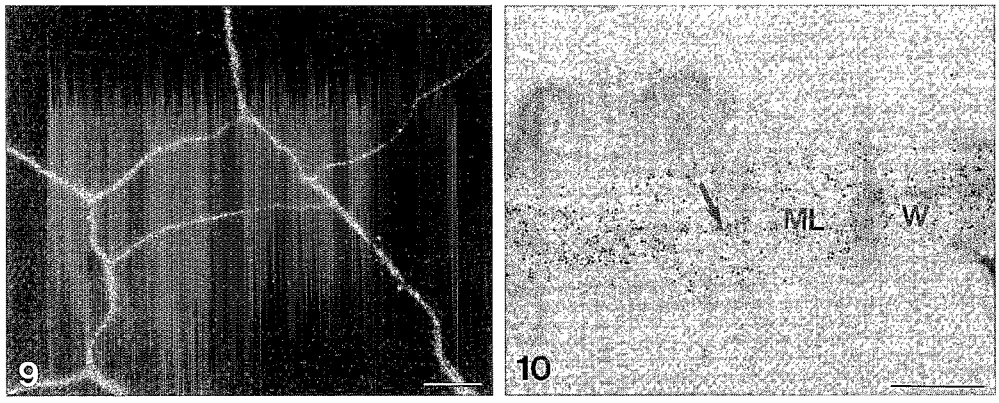


**Figs. 11–13.** Detection of pectins in the cell walls of secondary phloem parenchyma infected by *P. violae*, 96 h after inoculation. W, plant cell wall; H, hypha. Figure 11 shows cells colonized by *P. violae* (toluidine blue staining, immunogold labeling with JIM 5, silver intensification, bright field microscope observation). The cells contain hyphae, also located on a cell wall (arrow). Swollen cell walls are slightly stained, whereas others remain undegraded and stained. Scale bar = 10 μm. Figure 12 is the same section as in Fig. 11 but showing a regular brilliance over the undegraded cell walls (arrowhead), while the swollen portions are weakly brilliant (double arrowhead). When hyphae are located on the cell wall (arrow), no labeling is seen (immunogold labeling with JIM 5, silver intensification, epipolarized light microscope observation). Scale bar = 10 μm. Figure 13 shows details of a cell wall in contact with *P. violae* hyphae, after labeling with JIM 5 (large particles, 15 nm) and JIM 7 (small particles, 5 nm) (uranyl acetate and lead citrate staining). The labeling is irregular over the plant cell wall; no gold particles are seen over the cell wall close to the fungus, except over limited areas where only JIM 5 labeling is observed (arrow). Scale bar = 0.5 μm.

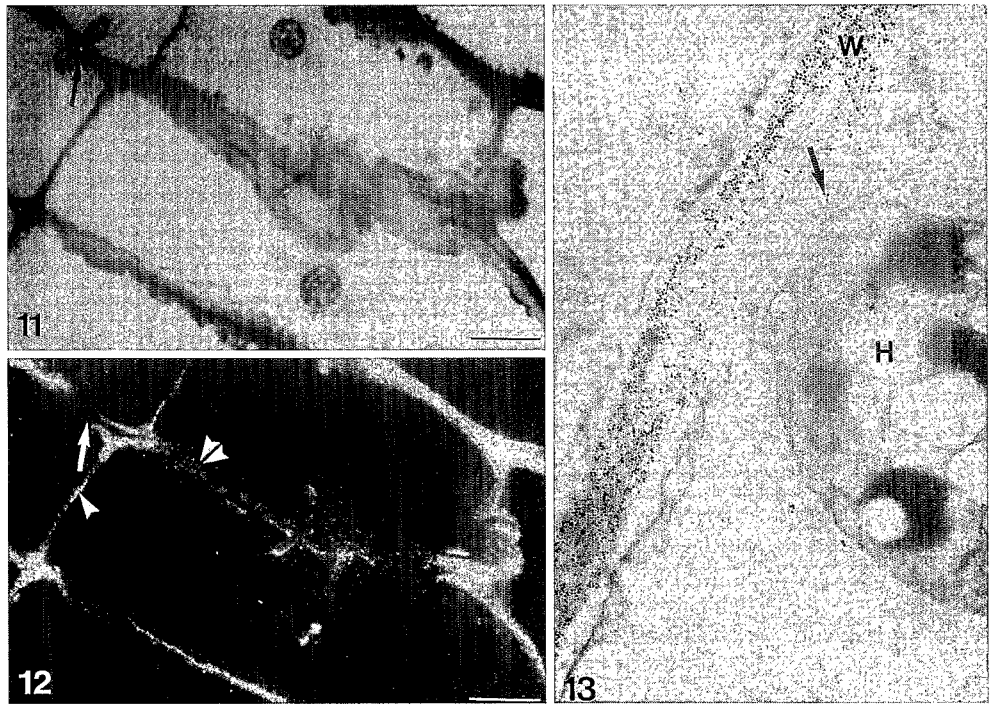


extensive degradations of cell walls, notably of pectins, than *P. violae*. The observation that cellulose appeared to be more intensely degraded after infection by *P. ultimum* than by *P. violae* could be related to (*i*) the higher cellulolytic activity and higher number of isoenzymes with cellulolytic activity observed in vitro (Campion et al. 1997) or (*ii*) easier access of cellulases to the polymer after alteration of the pectic matrix (Wood 1960). The undegraded intercellular junctions in totally degraded cell walls probably functioned as barriers before the whole loss of tissue integrity. This could be due to a lower

**Figs. 14–19.** Detection of pectins in the cell walls of secondary phloem parenchyma infected by *P. ultimum*, 96 h after inoculation. W, plant cell wall; C, plant cytoplasm; V, vacuole; H, hypha; J, intercellular junction. Figure 14 is a low magnification of the transition zone between a healthy area and an area infected by *P. ultimum* (toluidine blue staining, silver-intensified labeling with JIM 5, bright field microscope observation). Staining and labeling are localized over intercellular junctions and walls in unaltered areas. Few hyphae are present; they are seen only in the immediate vicinity of healthy tissues (arrow). Scale bar = 50 μm. Figure 15 shows details of the transition zone (toluidine blue staining, silver-intensified immunogold labeling with JIM 5, bright field microscope observation). Staining and labeling are almost absent over swollen cell walls but remain present over intercellular junctions (arrows). They are irregular over partially swollen cell walls and regular over the undegraded ones. Scale bar = 10 μm. Figure 16 is the same section as Fig. 15 but showing that the fluorescence mainly occurs over intercellular junctions of the swollen (arrow) or undegraded (arrowhead) cell walls. It is irregular over the partially swollen cell walls (double arrowhead) and wholly lacking over the swollen cell walls (silver-intensified immunogold labeling with JIM 5, epipolarized light microscope observation). Scale bar = 10 μm. Figure 17 shows details of an extensively swollen cell wall near a *P. ultimum* hypha after labeling with JIM 5 (small particles, 5 nm) and JIM 7 (large particles, 15 nm) and staining with uranyl acetate. No labeling is found over the cell wall, except over the intercellular junction (arrow). Scale bar = 2 μm. Figure 18 is an enlargement of the section in Fig. 17 showing the localization of the labeling with JIM 5 (arrow) and JIM 7 (arrowhead). Scale bar = 0.5 μm. Figure 19 shows the intercellular junction after labeling with JIM 5 (small particles, 5 nm) and JIM 7 (large particles, 15 nm) and staining with uranyl acetate. Labeling is uneven and weak over the less electron-opaque portion of the cell wall and intense over the more electron-opaque portion. Over the primary cell wall, the labeling is less intense than over the intercellular junction. Scale bar = 0.5 μm.

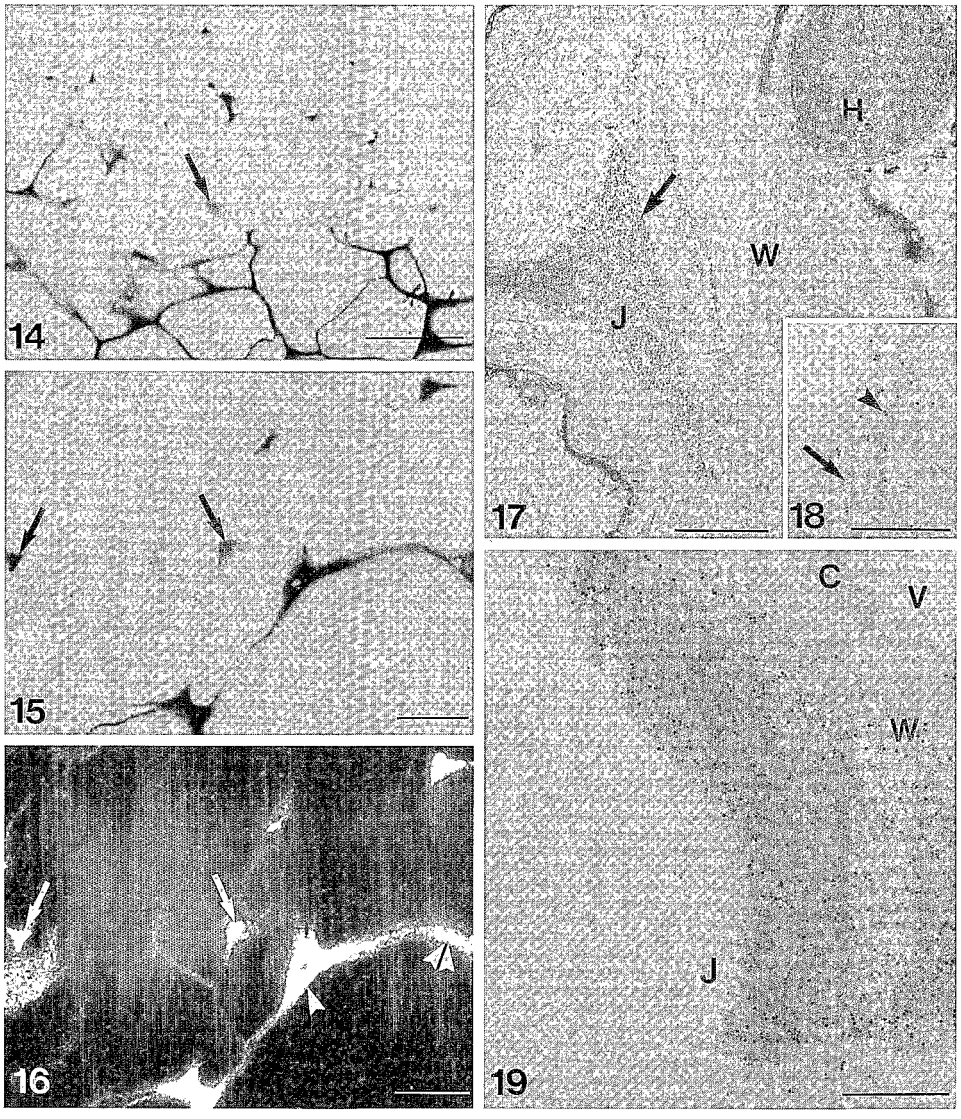


accessibility of the enzymes to their substrates in these areas or to reinforcement with calcium cations (Roy et al. 1994).

The cell wall degradations in the phloem parenchyma may explain the formation of cavities under the undegraded periderm. Compared with the disease owing to *M. acerina* (Davies et al. 1981), degradations apparently occurred in very limited areas,

**Figs. 20–24.** Detection of β-1,4-glucans, using an exoglucanase–gold probe in cell walls of the secondary phloem parenchyma in roots infected by *P. violae* and *P. ultimum*, 96 h after inoculation (transmission electron microscope observations). W, plant cell wall; C, plant cytoplasm; V, vacuole; H, hypha; J, intercellular junction. Scale bar = 1 μm. Figure 20 shows that in healthy roots, the labeling is regular over the cell wall (uranyl acetate and lead citrate staining). Figure 21 shows details of a cell wall in contact with two hyphae of *P. violae* (uranyl acetate staining). The labeling is distributed over the carrot and hyphal cell walls. It is particularly intense over the carrot cell wall areas close to the pathogen (arrow). The labeling is more intense over the cell walls of the altered tissues than of the unaltered ones. Figure 22 shows details of a totally swollen cell wall, where gold particles are regularly distributed over the primary cell wall (uranyl acetate and lead citrate staining). Figure 23 shows details of a totally swollen cell wall with a linear distribution of gold particles over the more lectron-opaque layer (arrow) (uranyl acetate and lead citrate staining). Figure 24 shows details of a partially swollen intercellular junction, where labeling is present over the less electron-opaque portion of the junction (arrow) and over the primary cell wall (arrowhead) but absent over the more electron-opaque portion of the junction (uranyl acetate and lead citrate staining).

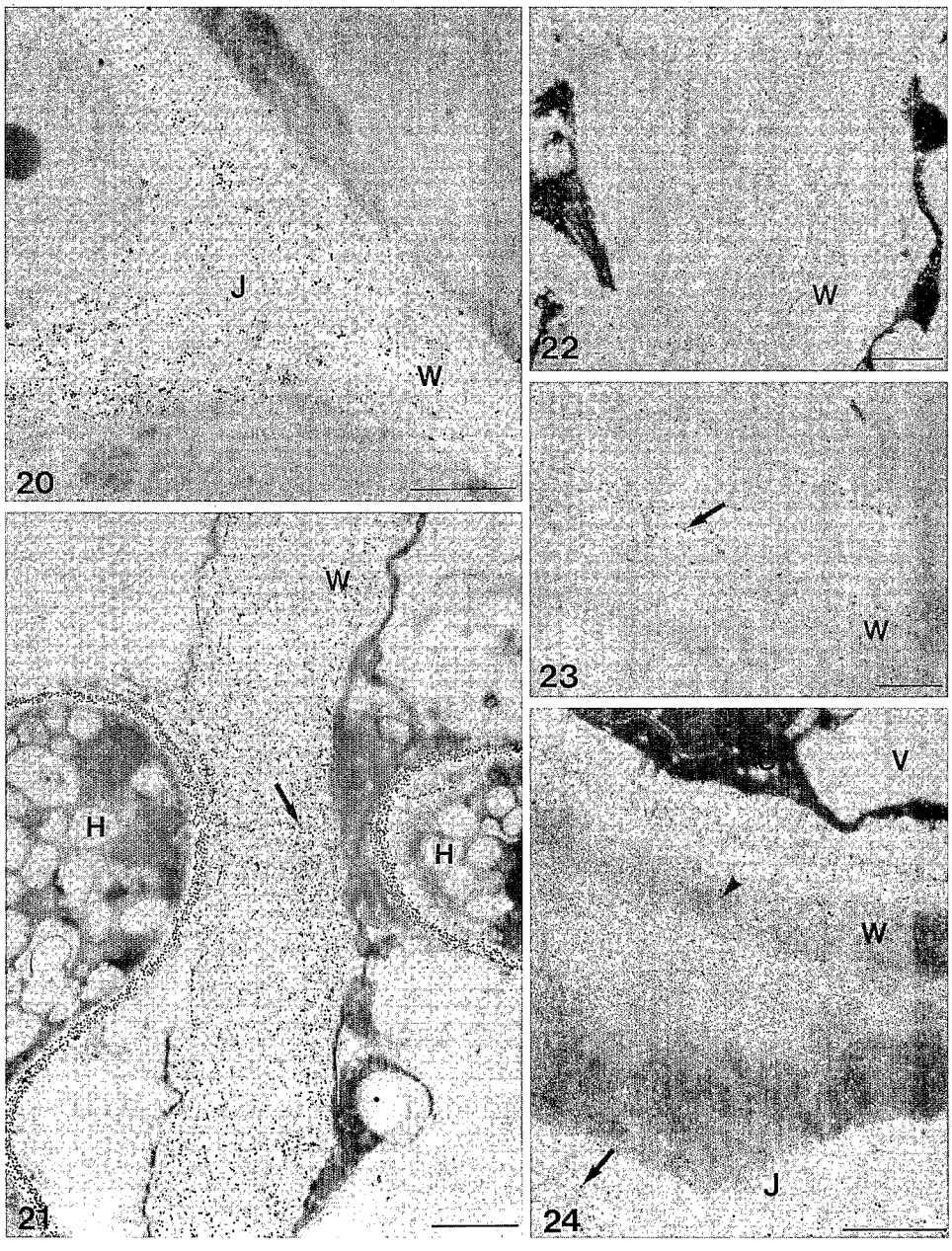


probably in relation to cell wall composition, in spite of differences in cell wall degradation by *P. violae* and *P. ultimum*. Changes in the cell wall organization owing to *P. ultimum* could be explained by higher activities for the degradation of cell wall polysaccharides, particularly pectins, detected in vitro for this species compared with *P. violae* (Campion

et al. 1997). We hypothesize that these higher activities detected for *P. ultimum*, associated with its rapid growth rate (Van der Plaats-Niterink 1981), explain these more intense degradations and, as a consequence, the larger and softer lesions.

The limited degradation of the cell walls, especially after infection, suggest that the enzymes have favourable sites for their action. This hypothesis is in agreement with the view of the cell wall as consisting of many limited domains varying in composition and structure (Roberts 1994) and could be verified by the localization of enzymes in situ. In this respect, localization of pectate lyase isoenzymes of *E. chrysanthemi* in *Saintpaulia ionantha* tissues was successfully undertaken with a specific monoclonal antibody (Temsah et al. 1991). In the same way, the use of a polyclonal serum permitted the localization and study of the complementary roles of two endo-polygalacturonases of *Sclerotinia sclerotiorum* in soybean hypocotyl tissues (Favaron et al. 1993). The use of labeling techniques to localize specific cell wall degrading enzymes within carrot tissues infected by *P. violae* or *P. ultimum* would be helpful to better understand the mechanisms by which the infection process of *Pythium* spp. operates to cause different symptoms in carrots.

In the same way, considering that phenolic compounds are accumulated and that enzymes involved in lignin-like compound synthesis are activated in carrot tissues after infection by *P. violae* (Zamski and Peretz 1995), an histological study of suberification and lignification would be useful to determine the evolution of cavity spot symptoms. This approach could indicate if defence reactions induced after infection by *P. violae* and *P. ultimum* are different, and so may account for the divergence of symptoms owing to the two pathogens.

## Acknowledgments

The authors are grateful to Dr K. Roberts for providing JIM 5 and JIM 7 monoclonal antibodies for the labeling experiments and to S. Roussel for technical assistance.

## References

Baker, C.J., Aist, J.R., and Bateman, D.F. 1980. Ultrastructural and biochemical effects of endopectate lyase on cell walls from cell suspension cultures of bean and rice. Can. J. Bot. **58**: 867–880.

Benhamou, N., Chamberland, H., Ouellette, G.B., and Pauzé, F.J. 1987. Ultrastructural localization of β-(1→4)-D-glucans in two pathogenic fungi and in their host tissues by means of an exoglucanase-gold complex. Can. J. Microbiol. **33**: 405–417.

Briard, I.M. 1990. Etude comparée de *Phytophthora megasperma* (Dresch.) et *Pythium violae* (Chest. & Hick.) et de leurs relations avec la plante dans l'expression des symptômes de bague et de cavity spot sur carotte (*Daucus carota*). Ph.D. thesis, University of Rennes I, Rennes, France.

Campion, C. 1997. Etude comparée des processus infectieux de *Pythium violae*, *Pythium sulcatum* et *Pythium ultimum* chez *Daucus carota* L. Rôles des enzymes fongiques et de la paroi végétale dans l'expression du cavity spot. Ph.D. thesis, University of Rennes I, Rennes, France.

Campion, C., Massiot, P., and Rouxel, F. 1997. Aggressiveness and production of cell-wall degrading enzymes by *Pythium violae*, *Pythium sulcatum* and *Pythium ultimum*, responsible for cavity spot on carrots. Eur. J. Plant Pathol. **103**: 725–735.

Chérif, M., Benhamou, N., and Bélanger, R.R. 1991. Ultrastructural and cytochemical studies of fungal development and host reactions in cucumber plants infected by *Pythium ultimum*. Physiol. Mol. Plant Pathol. **39**: 353–375.

Collmer, A., and Keen, N.T. 1986. The role of pectic enzymes in plant pathogenesis. Annu. Rev. Phytopathol. **24**: 383–409.

Davies, W.P., Lewis, B.G., and Day, J.R. 1981. Observations of infection of stored carrot roots by *Mycocentrospora acerina*. Trans. Br. Mycol. Soc. **77**: 139–151.

Deising, H., Heiler, S., Rauscher, M., Xu, H., and Mendgen, K. 1996. Cellular aspects of rust infection structure differentiation—spore adhesion and fungal morphogenesis. *In* Histology, ultrastructure and molecular cytology of plant–microorganism interactions. *Edited by* M. Nicole and V. Gianinazzi-Pearson. Kluwer Academic Publishers, Dordrecht, the Netherlands. pp. 135–156.

De Mey, J., Hacker, G.W., De Waele, M., and Springall, D.R. 1986. Gold probes in light microscopy. *In* Immunocytochemistry—modern methods and applications. 2nd ed. *Edited by* J.M. Block and S. Van Noordan. Wright, Bristol, U.K. pp. 71–88.

El-Tarabily, K.A., Hardy, G.E.ST.J., and Sivasithamparam, K. 1996. Association of *Pythium coloratum* and *Pythium sulcatum* with cavity spot disease of carrots in Western Australia. Plant Pathol. **45**: 727–735.

Favaron, F., Perotto, R., Bonfante, P., and Alghisi, P. 1993. Differential absorption and localization of two *Sclerotinia sclerotiorum* endo-polygalacturonases in soybean hypocotyls. Physiol. Mol. Plant Pathol. **43**: 353–364.

Groom, M.R., and Perry, D.A. 1985. Induction of 'cavity spot like' lesions on roots of *Daucus carota* by *Pythium violae*. Trans. Br. Mycol. Soc. **84**: 755–757.

Guérin, L. 1993. Analyse de la diversité des *Pythium* spp. impliqués dans le cavity spot de la carotte et étude des relations hôte-parasite en vue de la sélection variétale pour la résistance. Ph.D. thesis, University of Rennes I, Rennes, France.

Guérin, L., Briard, M., and Rouxel, F. 1994. Biochemical characterisation of *Pythium* spp. involved in cavity spot of carrots in France. Ann. Appl. Biol. **125**: 255–265.

Henrissat, B., Driguez, H., Viet, C., and Schulein, M. 1985. Synergism of cellulases from *Trichoderma reesei* in the degradation of cellulose. Bio/Technology, **3**: 722–726.

Kirtschev, N.A., and Kratchanov, C.G. 1980. Über Pektinstoffe einiger Vertreter der Art "*Daucus carota*". Z. Lebensm. Unters. Forsch. **170**: 31–33.

Knox, J.P., Linstead, P.L., King, J., Cooper, C., and Roberts, K. 1990. Pectin esterification is spatially regulated both within cell walls and between developing tissues of root apices. Planta, **181**: 512–521.

Le Cam, B., Lebreton, L., Massiot, P., and Rouxel, F. 1997. Production of cell-wall polysaccharide degrading enzymes in carrot root tissues infected by *Mycocentrospora acerina*. Plant Pathol. **46**: 276–281.

Massiot, P., Rouau, X., and Thibault, J.F. 1988. Characterisation of the extractable pectins and hemicelluloses of the cell wall of carrot. Carbohydr. Res. **172**: 229–242.

Montfort, F., and Rouxel, F. 1988. La maladie de la "tache" de la carotte due à *Pythium violae* Chesters et Hickman: données symptomatologiques et étiologiques. Agronomie, **8**: 701–706.

Roberts, K. 1994. The plant extracellular matrix: in a new expansive mood. Curr. Opin. Cell Biol. **6**: 688–694.

Roy, S., Vian, B., and Roland, J.C. 1992. Immunocytochemical study of the deesterification patterns during cell wall autolysis in the ripening of cherry tomato. Plant Physiol. Biochem. **30**: 139–146.

Roy, S., Jauneau, A., and Vian, B. 1994. Analytical detection of calcium ions and immunocytochemical visualization of homogalacturonic sequences in the ripe cherry tomato. Plant Physiol. Biochem. **32**: 633–640.

Sharman, S., and Heale, J.B. 1977. Penetration of carrot roots by the grey mould fungus *Botrytis cinerea* Pers. ex Pers. Physiol. Plant Pathol. **10**: 63–71.

Temsah, M., Bertheau, Y., and Vian, B. 1991. Pectate-lyase fixation

and pectate disorganization vizualized by immunocytochemistry in *Saintpaulia ionantha* by *Erwinia chrysanthemi*. Cell Biol. Int. Rep. **15**: 611–620.

Thiéry, J.P. 1967. Mise en évidence des polysaccharides sur coupes fines en microscopie électronique. J. Microsc. (Paris), **6**: 987–1018.

Touzani, A., and Donèche, B. 1996. Production et propriétés du complexe cellulasique du *Botrytis cinerea*. Can. J. Bot. **74**: 486–491.

VandenBosch, K.A., Bradley, D.J., Knox, J.P., Perotto, S., Butcher, G.W., and Brewin, N.J. 1989. Common components of the infection thread matrix and the intercellular space identified by immunocytochemical analysis of pea nodules and uninfected roots. EMBO J. **8**: 335–342.

Van der Plaats-Niterink, A.J. 1981. Monograph of the genus *Pythium*. *In* Studies in Mycology. Vol 21. *Edited by* W. Gams and R.P.W.M. Jacobs. Centraalbureau vor Schimmelcultures, Baarn.

Vivoda, E., Davis, R.M., Nunez, J.J., and Guérard, J.P. 1991. Factors affecting the development of cavity spot of carrot. Plant Dis. **75**: 519–522.

White, J.G. 1988. Studies on the biology and control of cavity spot of carrots. Ann. Appl. Biol. **113**: 259–268.

Wood, R.K.S. 1960. Pectic and cellulolytic enzymes in plant disease. Annu. Rev. Plant Physiol. **11**: 299–322.

Zamski, E., and Peretz, I. 1995. Cavity spot of carrots: interactions between the host and pathogen, related to the cell wall. Ann. Appl. Biol. **127**: 23–32.

Zamski, E., and Peretz, I. 1996. Cavity spot of carrots: II. Cell-wall-degrading enzymes secreted by *Pythium* and pathogen-related proteins produced by the root cells. Ann. Appl. Biol. **128**: 195–207.